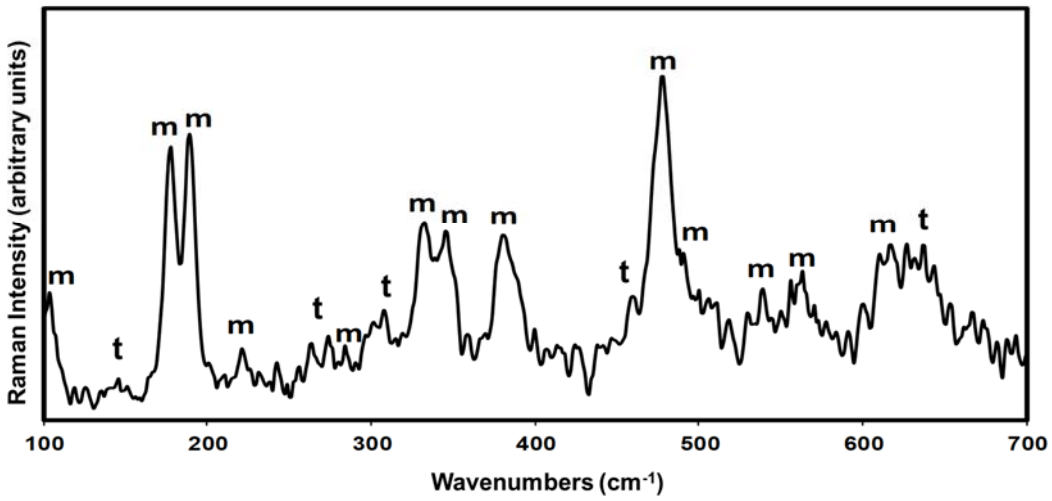

Fig. 1. Raman spectrum of ZrO_2 ceramic obtained by SPS at 350°C from $ZrOH_4$ precursor (m and t refer to monoclinic and tetragonal phases, respectively).

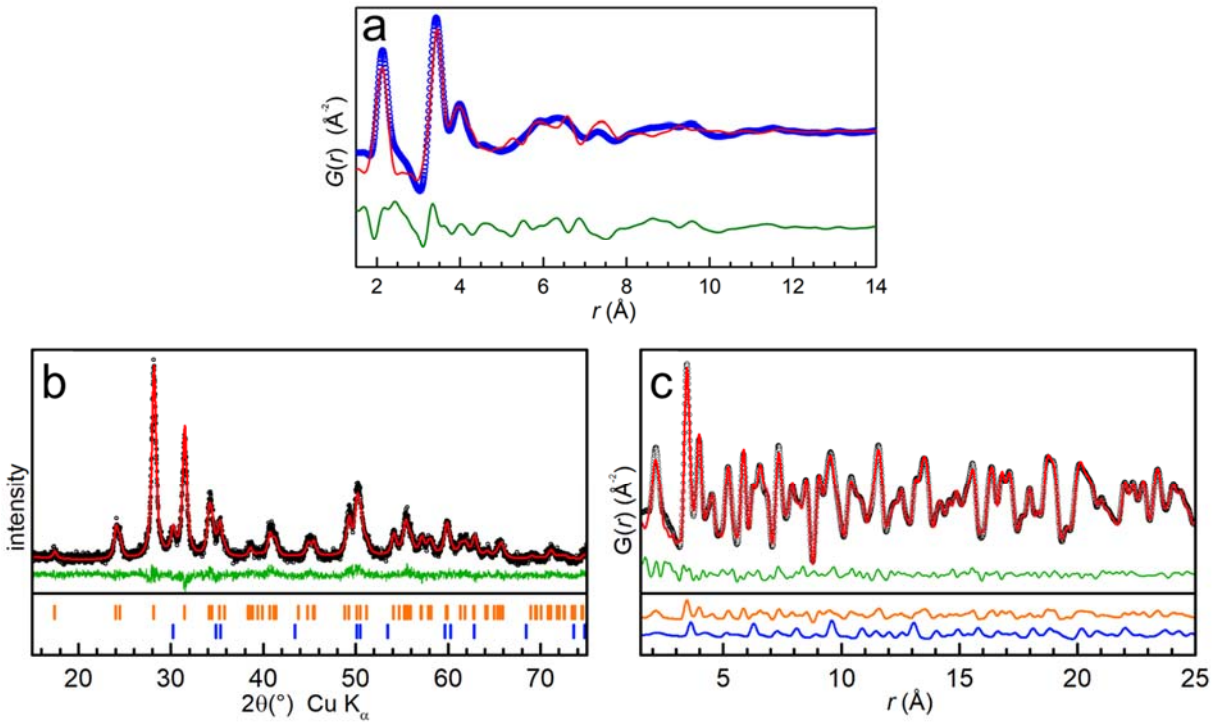

Fig. 2 a-c. a)Fit of G(*r*) for the $Zr(OH)_4$ reference powder using a monoclinic ZrO_2 structural model with a very small domain particle size < 10 Å. (*Rwp* = 35 %, refined in space group pace group $P2_{1/c}$ with *a* = 4.942(2) Å, *b* = 5.321(2) Å, c = 5.178(2) Å, and monoclinic angle β = 97.31(5)°. Experimental data are plotted as blue circles, with the calculated fit and difference curves as red and green lines, respectively.
b-c) Plots showing combined refined fit to powder XRD data (*b*) and PDF G(*r*) (*c*) for powder data measured on the SPS ceramic. Experimental data are shown as black circles, with the calculated fit and difference curves as red and green lines, respectively. For reference, for the XRD data (*a*) the lower panel shows 2θ position tick mark for monoclinic (orange) and tetragonal (blue) phases, while for the PDF data (*b*) simulated G(*r*) curves for monoclinic (orange) and tetragonal (blue) phases are plotted with compressed intensity scaling. (For interpretation of the references to color in this figure legend, the reader is referred to the web version of this article.).

	dataset	XRD		PDF	
	measurement	Cu-Kα PANalitycal X'pert		APS beamline 11-ID-B, 59 keV	
	weighting	1		18000	
	R_{wp}	8.3 %		12.9%	
Monoclinic ZrO_2 ($P2_1/c$)	*crystallite size (nm)*	15		12	
	phase fraction	0.93		0.95	
	lattice values	a = 5.1534(1) Å, b = 5.2088(1) Å, c = 5.3239(1) Å, β = 99.339(2)°			
	site	*x*	y	z	B_{iso} (Å^2)
	Zr1	0.27	0.04	0.21	0.6
	O1	0.07	0.33	0.34	1.0
	O2	0.45	0.76	0.48	1.0
Tetragonal ZrO_2 ($P4_2/nmc$)	*crystallite size (nm)*	12		11	
	phase fraction	0.07		0.05	
	lattice values	a = 3.6382(5) Å, c = 5.075(1) Å			
	site	*x*	y	z	B_{iso} (Å^2)
	Zr1	0	0	0	0.6
	O1	0	0.5	0.21	1.0

Table 1: Summary of combined PDF G(*r*) and XRD Rietveld refinements performed with the TOPAS V6 software, using a mixed monoclinic and tetragonal phase model, for powder data of the SPS ceramic. Lattice parameters and atomic positions for both phases were constrained across both datasets during the refinement. Note that listed B_{iso} values are from the XRD dataset fit; in the refined PDF model the B_{iso} values are similar but include an *r*-dependent broadening term. Crystallite size terms are refined separately for XRD and PDF data, as they are not equivalent size models. The combined fit has a total R_{wp} of 10.8%

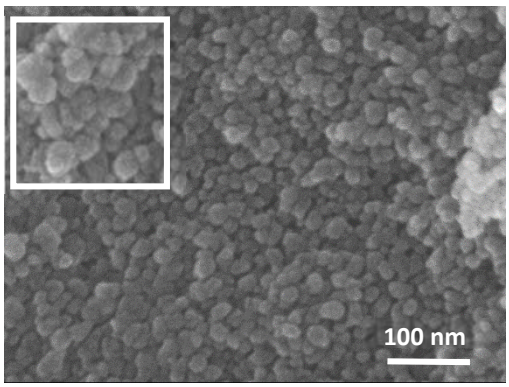

Fig. 3: HRSEM images of the fracture surface of the ZrO_2 ceramics processed by spark plasma sintering at 350°C °C starting from $ZrOH_4$ precursors. Insert: zoom on the formation of grain boundaries

Initial powder	Setpoint Temperature (°C)	Applied pressure MPa	Dwell time (min.)	Porosity (%)	% Polymorphs after SPS	Vickers Hardness (GPa)	Standard deviation
$ZrOH_4$ (US Nano)	350	600	10	~20-30	85(monoclinic) /15 (tetragonal)	3.805	14
6YSZ (Tosoh)	1050	50	1	34	100 (tetragonal)	3.462	11
5.1YSZ (sol gel)	1050	50	1	32.8	100 (tetragonal)	3.187	35

Table 2 Comparison of Vickers Hardness of zirconia SPS ceramics obtained from different precursors

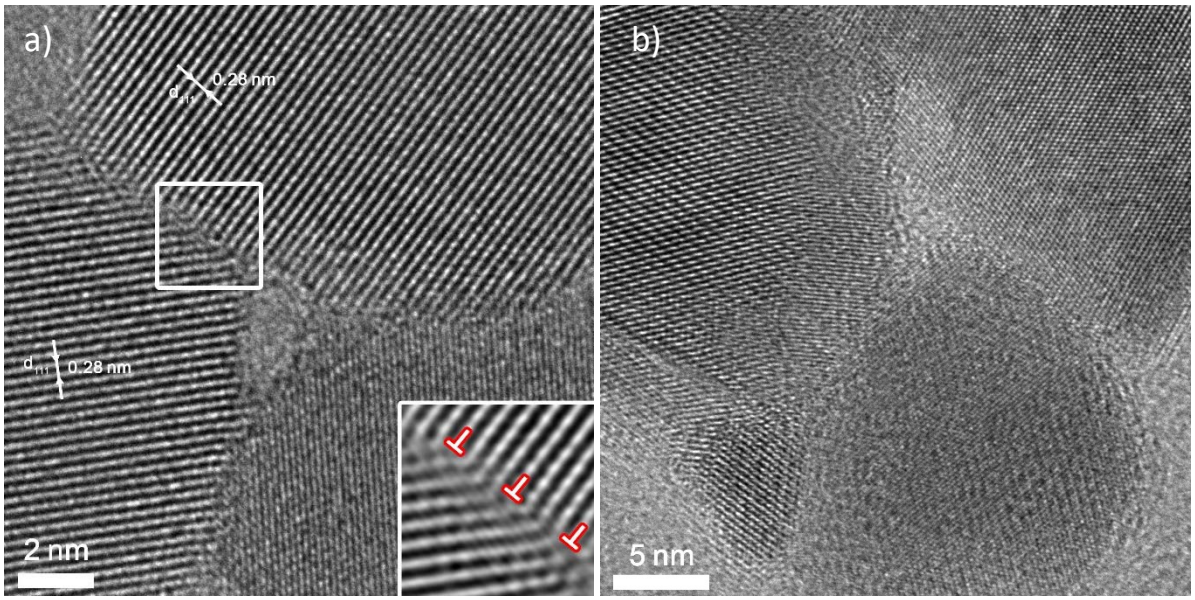

Figure 4 a) HRTEM micrograph of the sintered sample showing cavity nucleation at grain boundary triple junction and plastic interfaces highlighted by the presence of dislocation networks as shown on the inset (filtered image). **b)** HRTEM micrograph of grain boundary triple junctions formed by particles of different sizes or with cavity nucleation.